



COB-2021-1661 OBLIQUE SHOCK WAVE FOR AIR AT HIGH TEMPERATURE

Vinícius Lamas von Sohsten
Gabriel Afonso Pichorin
Pedro Paulo Batista de Araújo
George Santos Marinho
Paulo Gilberto de Paula Toro

Universidade Federal do Rio Grande do Norte (UFRN). Centro de Tecnologia. Av. Senador Salgado Filho, 3000 - Campus Universitário, Lagoa Nova CEP 59.078-970 – Natal/RN - Brasil
vinivon@gmail.com, gabrielpichorin@gmail.com, araujo.projects@gmail.com, gmarinho@ct.ufrn.br, toro11pt@gmail.com

Heidi Korzenowski

Universidade do Vale do Paraíba (UNIVAP). Faculdade de Engenharias, Arquitetura e Urbanismo. Av. Shishima Hifumi nº 2911. Urbanova. CEP 12.224-000 São José dos Campos/SP – Brasil
heidi@univap.br

Abstract. Academically, the oblique shock wave relationships are obtained considering, the inviscid flow (no boundary layer effects) and the airflow behaves as a calorically perfect gas (no high temperature effects). In general, for an aerospace vehicle design using airbreathing propulsion, based on supersonic combustion (scramjet technology), the analytical methodology is applied. The scramjet vehicle flying, in a dense Earth atmospheric air, in hypersonic velocity, oblique shock waves are established, promoting high temperature of the airflow that experiment the oblique shock waves, enough to generate air (oxygen and/or nitrogen) dissociation. Therefore, oblique shock relations for air in thermodynamic equilibrium are developed, and validated by academic literature available and applied to scramjet vehicle, with leading-edge (turning) deflection angle of 20° and 30°, flying at hypersonic velocities, corresponding to Mach numbers 7 and 10, at 30 km altitude. The results for the pressure, temperature and density ratios and flow deflection across the shock wave are presented as function of the shock wave angle and airflow velocities. Oblique shock relations for perfect gas airflow and airflow in thermodynamic equilibrium are compared.

Keywords: *oblique shock wave, air in equilibrium, analytical analysis, scramjet inlet.*

1. INTRODUCTION

An aerospace vehicle integrated with a hypersonic airbreathing propulsion system, based on supersonic combustion (scramjet technology), can achieve hypersonic speed, that is, at least five times the speed of sound. Basically, scramjet is a fully integrated airbreathing aeronautical engine, with no moving parts, that uses the oblique/conical shock waves generated during the hypersonic flight. The scramjet may be divided in three main components (Fig. 1): external and internal compression section (inlet), combustion chamber (combustor), and internal and external expansion section (outlet) (Heiser and Pratt, 1994).

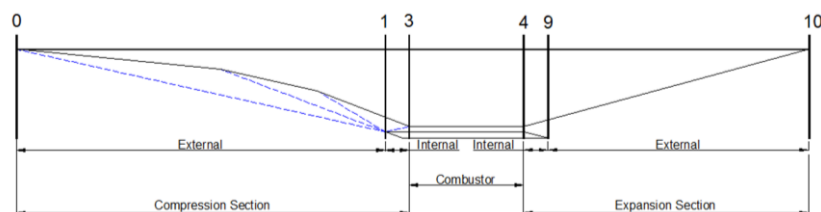


Figure 1. Airframe-integrated scramjet engine stations and reference terminology, adapted from Heiser and Pratt (1994).

The compression section provides the compression and deceleration of freestream atmospheric air at the inlet of the scramjet, stations 0 to 3 (Fig. 1), which are pushed to combustion chamber, stations 3 to 4. Fuel is injected into the supersonic airflow at the beginning of the combustion chamber (combustor). After mixing of oxygen (from the atmospheric air) and on-board (in general, hydrogen) fuel, both fuel-oxygen are burned. Finally, the divergent exhaust nozzle, stations 4 to 10, at the after body vehicle accelerates the exhaust gases, providing thrust (Toro *et al.*, 2018a).

Due to the high speed, the temperature promoted by the oblique shock wave caused by the scramjet is also quite high, causing chemical reactions in the gas. Reactions such as dissociation of oxygen and nitrogen molecules into oxygen and nitrogen atoms from a temperature of 2000 K for the first and 4000 K for the second, formation of nitrogen oxide from approximately 6000 K and even ionization at temperatures higher than 9000 K (Anderson, 2006).

Toro *et al.* (2018a; 2018b) designed a generic two-dimensional hydrogen-powered scramjet, at the Universidade Federal do Rio Grande do Norte (UFRN), using an engineering approach, to demonstrate, during atmospheric flight, the supersonic combustion of atmospheric airflow (at supersonic speed) with hydrogen, when the scramjet vehicle is at 2050 m/s (corresponding to Mach number 6.8) at 30 km altitude. In this design, the shock wave theory, the one-dimensional (Rayleigh) flow with heat addition theory, and the expansion wave (Prandtl-Meyer) theory coupled with the area ratio theory, can describe several characteristics of the compression section, the combustion chamber section and the expansion section, respectively, of the hypersonic airbreathing vehicle. The theories, considering air as a calorically perfect gas (with no high temperature effects) and inviscid flow (without the boundary layer effects), are used to estimate the thermodynamic properties (pressure, temperature, density, sound velocity) and velocities (corresponding to Mach numbers) of the supersonic airflow, from the leading-to-trailing edges of the supersonic combustion (scramjet) demonstrator. One of the most important aspects of the design is the temperature and velocity of the atmospheric air at the entrance to the combustion chamber, provided by the compression section. The airflow temperature, at the entrance of the combustion chamber, must be sufficiently high, higher than the hydrogen ignition temperature, in supersonic velocity for supersonic combustion to occur. In addition, airflow mass and hydrogen flow mass rates are critical design parameters to burn stoichiometrically hydrogen-airing supersonic velocity at the combustion chamber, to generate high velocity combustion products at the trailing-edge of the generic scramjet in order to produce thrust.

Chark *et al.* (2006) presented a (two-dimensional) design of a hypersonic vehicle integrated with scramjet (burning hydrogen), under development at the Multidisciplinary Flight Dynamics and Control Laboratory, of California State University, Los Angeles (USA), with the objective of carrying out missions for both access to space and for military applications, for flight in the Earth's atmosphere at an altitude of 30 km altitude at hypersonic speed, corresponding to Mach number 10. Studies on aerodynamics (using analytical methodology), aerodynamic parameters (numerical methodology) and the system propulsion systems were used to develop the control challenges associated with the scramjet. Theories of oblique shock wave, of heat addition in one-dimensional (Rayleigh) flow and of expansion (Prandtl-Meyer) wave were applied in the compression, combustion and expansion sections, respectively, aiming to determine the thermodynamic properties (pressure, temperature, density) and velocity (Mach number) of the airflow that experienced the establishment of oblique shock wave, the addition of heat and the establishment of the expansion wave. Aerodynamic forces (lift, drag and thrust) were estimated based on the change in Momentum of the flow in the three sections (compression, combustion and expansion).

Hariramakrishnan *et al.* (2017) presented a computational analysis for the inlet section of the scramjet vehicle. Results demonstrated this geometry is capable to generate flow for a steady combustion on the combustion chamber. In this paper, compression geometry was determined after shock wave interaction calculations and sketched using software CATIA V5. Numerical study is divided in three components: a) the pre-processing, where the geometry and mesh were generated and the boundary conditions were implemented in the software; b) the simulation, done by the solver tool, where discretization and linearization were used to find an approximated solution; and c) post processing, where results were presented for the user. The analysis was done for flight Mach number 7 and altitudes of 11 km, 20 km and 25 km in Earth's atmosphere. Two ramp angles were chosen for the vehicle, 9° and 20.5° for the first and the second ramps, respectively. Density and temperature were assumed constant while pressure decreases with altitude.

Bonelli *et al.* (2011) presented a scramjet design to fly with a speed corresponding to Mach number 7.5, in the altitude of 30 km. Three cases were considered: a) considering scramjet design without hydrogen-air combustion, disregarding the viscous effects and including air dissociation; b) considering scramjet design without combustion, but considering the viscous effects and the air modeled as calorically perfect and assuming freezing conditions; c) considering combustion in the scramjet engine, assuming chemically reactive gas in non-equilibrium and neglecting the viscous effects. The analyzes showed that when including the viscous effects there is a good agreement between the results obtained using the SPREAD 2.0 code and the CFD for the predictions of the distribution of pressure, temperature and hydrogen mass fraction along the axial direction. The satisfactory results confirmed that the SPREAD 2.0 code was a powerful tool for primary analysis of scramjet design, reducing costs and time associated with the massive use of CFD or experimental tests.

This paper presents the model and methodology used to calculate the ratios of thermodynamic properties through the oblique shock wave considering both the perfect gas and the real gas airflow. For perfect gas, only the analytical method described in Anderson (2003) were used to perform the calculations directly. As for the real gas, considering air in chemical and thermodynamic equilibrium the method presented in Tannehill and Mugge (1974) were used, which performs the calculations of the ratios by the process of polynomial correlation, using tabulated and calculated coefficients.

The method presented in Tannehill and Mugge (1974) was, first, developed for equilibrium properties of high-temperature airflow after normal shock waves, and was adapted for airflow in equilibrium after oblique shock wave.

The algorithm developed to solve the modified Tannehill and Mugge (1974), in the present paper, was written in Python platform. The results were validated based on: a) Moura and Pinheiro Rosa (2013) data and b) Moeckel (1957). Finally, the present procedure was applied to scramjet, with only one ramp, flying and velocities corresponding to Mach numbers 7 and 10 at 30 km of geometric altitude, with the leading-edge deflection angles of 20° and 30°.

2. METHODOLOGY

2.1 Oblique shock wave theory

Shock waves are physical phenomena in fluids that are established when the flow with high velocities, greater than the local speed of sound, meets a wedge with a positive angle, where sudden the values of thermodynamic properties (pressure, temperature, and density) increase, consequently the flow velocity (and corresponding Mach number) decreases.

The incoming flow is denoted by the subscript “1”, and subscript “2” represents the flow after the oblique shock wave. In this case, the flow is in two-dimensional. The velocity vector V_{in} can be decomposed into normal and tangential velocity components, subscripts “n”, and “t”, respectively. As the flow approaches a sharp wedge, it is deflected by an angle θ and remains parallel to the surface of the body. This disturbance generates an oblique shock of angle β greater than the deflection angle, which compresses the flow. Anderson (2003) presented the shock wave relationship, considering steady state, inviscid (no boundary layer effects) and adiabatic compressible flow.

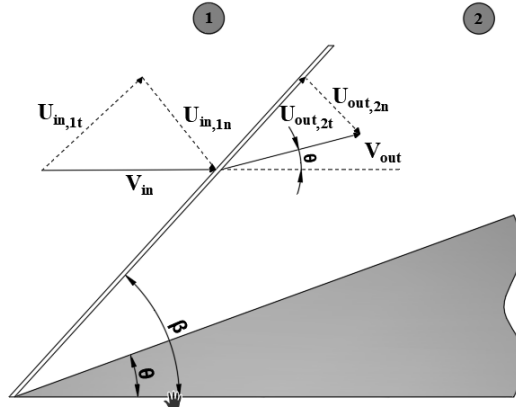


Figure 1. Schematic of flow through an oblique shock (Toro *et al.*, 2018a).

$$\rho_1 u_{1n} = \rho_2 u_{2n} \quad (1)$$

$$p_1 + \rho_1 u_{1n}^2 = p_2 + \rho_2 u_{2n}^2 \quad (2)$$

$$u_{1t} = u_{2t} \quad (3)$$

$$h_1 + \frac{u_{1n}^2}{2} = h_2 + \frac{u_{2n}^2}{2} \quad (4)$$

where:

$$u_{1n} = u_1 \sin \beta \quad (5)$$

$$u_{2n} = u_2 \sin(\beta - \theta) \quad (6)$$

and where: ρ , p , u and h are density, pressure, velocity, and enthalpy of the gas across the oblique shock wave, respectively. These equations hold for any type of gas since no gas model was used in the assumptions for the study of a shock wave. In the following sections it will be discussed how to better fit those equations for applications in both ideal and equilibrium gas flow.

2.2 Oblique shock wave relationships for calorically perfect gas

According to Anderson (2006), calorically perfect gas is a theoretical gas in which particle size, interactions and forces are not significant. Atmospheric air behaves as calorically perfect gas under high temperatures and low pressure.

Specific heats are assumed constant, and internal energy and enthalpy behaves as a linear function of temperature for ideal gases. Considering inviscid, steady, adiabatic flow and for calorically perfect gas the shock wave angle β is a function of the flow deflection angle θ , the incoming Mach number M_1 , the heat capacity ratio γ through the following relationship.

$$\tan \theta = 2 \cot \beta \left[\frac{M_1^2 \sin^2 \beta - 1}{M_1^2 (\gamma + \cos 2\beta) + 2} \right] \quad (7)$$

Manipulating governing equations 1 to 6 for the calorically perfect gas hypothesis across an oblique shock flow Mach number and the thermodynamic property ratios are functions of the normal component of the free stream velocity as follows.

$$M_{2n}^2 = \frac{1 + \frac{\gamma-1}{2} M_{1n}^2}{\gamma M_{1n}^2 - \frac{\gamma-1}{2}} \quad (8)$$

$$\frac{p_2}{p_1} = 1 + \frac{2\gamma}{(\gamma + 1)} (M_{1n}^2 - 1) \quad (9)$$

$$\frac{\rho_2}{\rho_1} = \frac{M_{1n}^2 (\gamma + 1)}{[2 + (\gamma - 1) M_{1n}^2]} \quad (10)$$

$$\frac{T_2}{T_1} = \frac{\frac{p_2}{p_1}}{\frac{\rho_2}{\rho_1}} \quad (11)$$

where:

$$M_{1n} = M_1 \sin \beta \quad (12)$$

These relationships show that pressure, temperature and density increase after the shock wave and the Mach number (and corresponding flow velocity) decreases, but the flow remains supersonic and parallel with the inlet surface of the scramjet.

2.3 Oblique shock wave relationships for air in thermodynamic equilibrium

As a gas is compressed through a shock wave temperature increases very rapidly in an abrupt manner, under these conditions specific heats are not expected to be constant, therefore calorically perfect gas assumptions do not represent high velocity flow. According to Anderson (2006) as flow velocities increases and the gas after shock waves reaches higher temperatures, other thermodynamic effects, such as vibrational excitation and dissociation, on the flow must be considered for accuracy on calculation over ideal gas theory.

Tannehill and Muge (1974) developed a method based on polynomial equations and tabulated data to retrieve thermodynamic properties of air in equilibrium from two intensive local properties of the flow, and applied to a normal shock wave. These equations were corrected to fit predicted data from statistical thermodynamics for atmospheric air. Tannehill and Muge method for specific enthalpy and temperature functions of flow pressure and density represented as:

$$h = \frac{p}{\rho} \left[\frac{\tilde{\gamma}}{\tilde{\gamma} - 1} \right] \quad (13)$$

$$\tilde{\gamma} = c_1 + c_2 Y_1 + c_3 Z_1 + c_4 Y_1 Z_1 + \frac{c_5 + c_6 Y_1 + c_7 Z_1 + c_8 Y_1 Z_1}{1 + \exp[c_9 (X_1 + c_{10} Y_1 + c_{11})]} \quad (14)$$

where:

$$X_1 = \log \left(\frac{P}{1.013 \times 10^5} \right); Y_1 = \log \left(\frac{\rho}{1.292} \right); \text{ and } Z_1 = X_1 - Y_1 \quad (15)$$

and

$$\log\left(\frac{T}{151.78}\right) = d_1 + d_2 Y_2 + d_3 Z_2 + d_4 Y_2 Z_2 + d_5 Z_2^2 + \frac{d_6 + d_7 Y_2 + d_8 Z_2 + d_9 Y_2 Z_2 + d_{10} Z_2^2}{1 + \exp[d_{11}(Z_2 + d_{12})]} \quad (16)$$

where:

$$X_2 = \log\left(\frac{P}{1.0134 \times 10^5}\right); Y_2 = \log\left(\frac{\rho}{1.225}\right); \text{ and } Z_2 = X_2 - Y_2 \quad (17)$$

The coefficients c_i and d_i on Eq. (14) and Eq. (16), respectively, are tabulated in Tannehill and Mugge (1974). The manipulated governing equations (1, 2 and 4) were applied for the air in equilibrium:

$$u_{2n} = \frac{\rho_1 u_{1n}}{\rho_2} \quad (18)$$

$$p_2 = p_1 + \rho_1 u_{1n}^2 \left(1 - \frac{\rho_1}{\rho_2}\right) \quad (19)$$

$$h_2 = h_1 + \frac{u_{1n}^2}{2} \left[1 - \left(\frac{\rho_1}{\rho_2}\right)^2\right] \quad (20)$$

$$\tan(\beta - \theta) = \frac{u_{2n}}{u_{1n}} \tan \beta \quad (21)$$

2.4 Algorithm for numeric solution

Once it is known Earth's atmosphere conditions at a given altitude and given Mach number, the Eq. (19) and (20) express p_2 and h_2 in function of ρ_1/ρ_2 and β is function of equation of u_{2n} and u_{1n} . This lays the foundation for the iterative numerical solution, which is done through the following steps:

- 1) Arbitrate a value for u_{2n}/u_{1n} (a value of 0.1 is normally good for a start).
- 2) Using secant method, obtain a value for β , for a given θ , using Eq. (21).
- 3) Arbitrate a value for ρ_1/ρ_2 . (a value of 0.1 is normally good for a start).
- 4) With the calculated values of p_2 and h_2 , calculate \tilde{Y} Eq. (14).
- 5) Calculate ρ_2 from Eq. (13) to obtain a new value for ρ_1/ρ_2 .
- 6) Use the new value of ρ_1/ρ_2 to obtain new values for p_2 and h_2 . Then repeat steps 4 to 6 until convergence is achieved, that is, until the value of ρ_1/ρ_2 between two consecutive iterations is practically equal.
- 7) Calculate the new value of u_{2n} from Eq. (18) using the new ρ_1/ρ_2 .
- 8) With the new value of u_{2n}/u_{1n} , use secant method to obtain a new value for β , using Eq. (21). Then repeat steps 3 to 8 until convergence is achieved, that is, until the value of β between two consecutive iterations is practically equal.
- 9) With the correct values of β , u_{2n} , ρ_2 , p_2 and h_2 , calculate T_2 from Eq. (16) and u_2 .

Following steps 1 to 9 as described, with a given flow condition in front of the shock wave, it is possible to obtain all properties and ratios across the shock wave.

3. RESULTS

The program was developed using Python 3 programming language, versatile and useful for numerical calculations, such as oblique shock wave relations. First, to validate the algorithm, the experimental data and approximate results from the graphs presented by Moura and Pinheiro Rosa (2013) were used, with the input values and the airflow deflection angle θ of 30° (Fig. 1) presented in Table 1.

Moura and Pinheiro Rosa (2013) presented the developed computer code to calculate airflow conditions behind normal and oblique shock waves considering two distinct gas models for the air: a) calorically perfect and b) chemical and thermodynamic equilibrium. In the chemical and thermodynamic equilibrium, high temperature effects in the air such as molecular vibration and dissociation and atomic ionization are taken into account by using the mathematical correlations given by Srinivasan *et al.* (1987). Assuming the pressure, temperature and Mach number of the airflow at free stream are known, it is possible to obtain the results for the airflow conditions behind a normal and/or oblique shock wave. Moura and Pinheiro Rosa (2013) validated the oblique shock wave calculations, with data from Nagamatsu (1960), with input values given in Table 1, while varying the deflection angle θ .

Nagamatsu *et al.* (1960) presented the oblique shock relations for dissociated air for a free stream flow Mach number of 7.8 with an equilibrium stagnation temperature of 7200 R in the reservoir of the test section of Rensselaer Polytechnic Institute Hypersonic Shock Tunnel. The results for the flow deflection across the shock wave and temperature, pressure, density ratios were presented as functions of the shock wave angle. The equilibrium airflow of oblique shock relations was experimentally verified by testing an adjustable two-dimensional wedge model in a hypersonic shock tunnel.

Table 1. Input values, used for validation, presented by Moura and Pinheiro Rosa (2013).

Mach number	7.8
Temperature	450.0 K
Pressure	142.032 Pa

The developed algorithm was validated only considering the airflow deflection angle θ of 30° . One may observe the comparison was quite good, Table 2, despite of the difficulty to extract the data from the Moura and Pinheiro Rosa (2013) and Nagamatsu *et al.* (1960) the approximate results, taken from graphs, for flow deflection angle of 30° .

Table 2. Conditions after oblique shock wave from Moura and Pinheiro Rosa (2013) and Nagamatsu *et al.* (1960).

	Mach number behind shock	Shock wave angle	Temperature ratio	Density ratio	Pressure ratio
Moura and Pinheiro (2013)	not presented	37.7°	4.70	5.8	27.4
Nagamatsu <i>et al.</i> (1960)	3	37°	4.85	5.9	27.7
Present results	2.976	37.471°	4.804	5.845	27.130

For multiple values of deflection angle and free stream velocities a range of shock wave angles are the solutions for equations (7) and (20), to the respective air model (Figure 2).

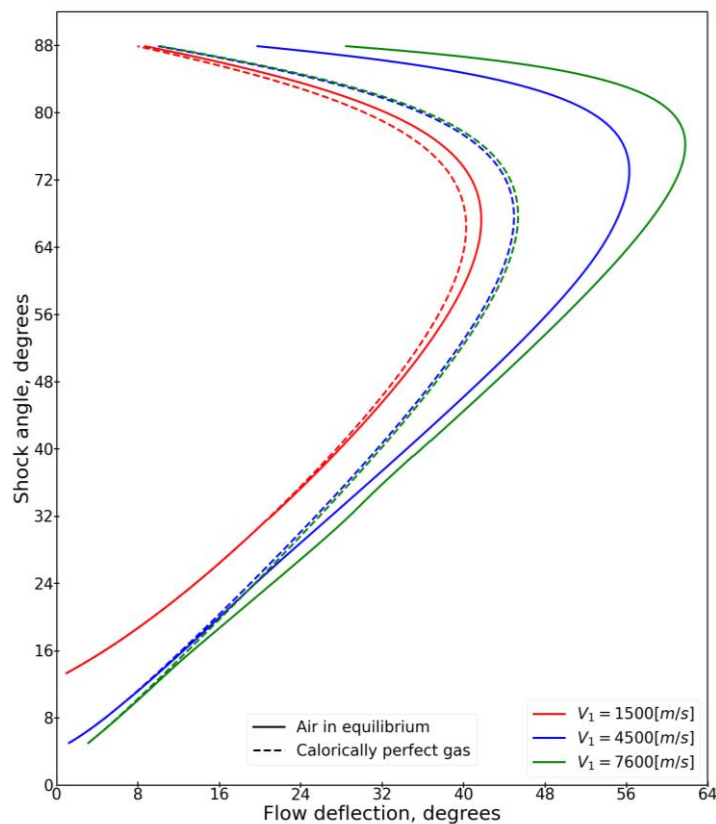


Figure 2. Deflection angle, shock wave angle, velocity diagram for oblique shock at 30.5 km altitude.

Two shock angles are possible for the same deflection, a stronger, more vertical shock, where thermodynamic properties ratios are higher through the flow, and a weaker more horizontal shock, with lesser increase in pressure,

temperature, and density. Stronger shock usually forms only when energy is added to the flow as it approaches the wedge, hence further discussion will only focus on the weak shock solution since the flow is considered adiabatic. Higher deflection angles produce a stronger shock (β increases with θ) in the flow up to a maximum deflection, any further increase in deflection leads to a bow shock detached from the wedge, where oblique shock theory is no longer valid.

Across velocities of 1500 m/s, 4500 m/s and 7600 m/s at 30.5 km of geometric altitude (Figure 2), shock waves formed in air in equilibrium are weaker when compared to the calorically perfect gas solution. This is observed because energy is absorbed by molecular and chemical effects in high energy gas flow. Since velocity is a factor for total enthalpy, differences between ideal and real gas models are better noticed on higher velocities. As upstream velocity increases the shock approaches the wedge surface, the disturbance in flow is not enough to decelerate the faster incoming air leading to a higher tangential velocity in the shock, therefore forming weaker shock.

Following, the pressure, temperature and density ratios and the oblique shock wave were estimated applying the oblique shock wave relations considering the Earth's atmosphere conditions at an altitude of 30 km, Table 3, obtained from U.S. Standard Atmosphere (1976).

Table 3. Thermodynamic atmospheric properties at 30 km altitude (U.S. Standard Atmosphere, 1976).

Altitude	Temperature	Pressure	Density	Sound speed
km	K	Pa	kg/m ³	m/s
30	226.5	1197	0.01841	301.7

For calorically perfect gas airflow, with $\gamma = 1.4$, the results were easily obtained by just applying the equations and the values presented in Table 4. Considering the air in chemical and thermodynamic equilibrium, the thermodynamic property ratios (pressure and temperature) and shock wave were calculated for an altitude of 30 km and Mach number 7 and 10, as presented in Table 4.

As one may observe for Mach 7 and deflection angle 20°, the high temperature is not too strong as Mach number increased to Mach number 10. However, for a deflection angle of 30°, the influence of high temperature is stronger.

Table 4. Property ratios across the shock wave for calorically perfect gas and air in equilibrium.

θ		Mach	$\frac{p_2}{p_1}$	$\frac{T_2}{T_1}$	β
20°	calorically perfect gas	7	11.8402	2.9321	27.2771
	air in equilibrium	7	11.7686	3.0066	27.0942
	calorically perfect gas	10	21.9614	4.6251	25.8178
	air in equilibrium	10	21.6651	4.5407	25.4442
30°	calorically perfect gas	7	23.3101	4.8503	39.8543
	air in equilibrium	7	22.9174	4.7306	39.1179
	calorically perfect gas	10	45.0794	8.4818	38.5175
	air in equilibrium	10	43.9296	7.8091	37.4521

Table 5 presents the pressure, temperature considering air as calorically perfect gas and air in equilibrium. For hypersonic vehicle design based in supersonic combustion propulsion system (scramjet technology) the influence of high temperature (dissociation phenomena) is not too strong, thereby the preliminary scramjet design may use calorically perfect gas relationships.

Table 5. Thermodynamic properties behind oblique shock wave at Mach numbers 7 and 10.

Properties across the shock wave	θ	Mach number 7		Mach number 10	
		p_2	T_2	p_2	T_2
Perfect gas airflow	20°	14173.16 Pa	664.14 K	26288.52 Pa	1047.63 K
Air in thermodynamic equilibrium		14087.39 Pa	681.03 K	25933.80 Pa	1028.51 K
Perfect gas airflow	30°	27902.89 Pa	1098.65 K	53961.36 Pa	1921.22 K
Air in thermodynamic equilibrium		27432.89 Pa	1071.53 K	52585.00 Pa	1768.84 K

4. CONCLUSION

The understanding of shock wave theory in different mediums is important for applications in different aerospace technologies, such as scramjet, shock tubes and rockets. Research and investments in this field leads to a stronger aerospace industry, up to date with latest discoveries, technologic development and applications. Therefore, mastering gas behavior calculations in more complex physics are necessary. Equilibrium gas dynamics through Tannehill and Mugge method give a more robust analysis of high velocity flows through shock waves, where molecular effects are taken into consideration on the calculation, hence better fitting real gas behavior expected in atmospheric flight than the calorically perfect gas consideration.

A computer program, using Python programming language, was developed to aid hypersonic compressible gas flow calculations in Earth's atmosphere as the fluid experiences an oblique shock wave. The program followed the conservation laws of continuity, momentum and energy for calorically and equilibrium adiabatic, two dimensional, steady and non-viscous flow. The numerical approach used for convergence was the secant method on iterations until the error was insignificant for the analysis. This code was used to simulate atmospheric flight of scramjet under Mach numbers of 7 and 10 at 30 km of geometric altitude.

Results for the numerical analysis agreed with data from literature. Expected increase in thermodynamic properties and decrease in flow velocity were observed for both calorically perfect gas and air in equilibrium. Results demonstrate that ideal gas considerations lead to a stronger shock wave than equilibrium air; this is because energy is not absorbed by molecular phenomenon not considered on the analysis. These errors are conservative and provided a sufficiently approach to preliminary design of aerospace vehicle based on supersonic combustion propulsion system, done under calorically perfect gas behavior.

5. ACKNOWLEDGEMENTS

This study was financed in part by the Coordenação de Aperfeiçoamento de Pessoal de Nível Superior - Brasil (CAPES) - Finance Code 001. The authors would like to thank the Universidade Federal do Rio Grande do Norte (UFRN) to support granted to carry out research on equilibrium properties of high-temperature air. Also, the second author would like to thank the CAPES for the Master scholarship from the Project PROCAD-DEFESA 88887.626266/2021-00. Finally, the fourth author thanks the Universidade do Vale do Paraíba (UNIVAP).

6. REFERENCES

- Anderson Jr., J. D. (2003) *Modern Compressible Flow: with Historical Perspective*. McGraw-Hill series in Aeronautical and Aerospace Engineering. Third Edition. ISBN 0-07-242443-5. ISBN 0-07-1 12161-7 (ISE).
- Anderson, J. D. (2006). *Hypersonic and High Temperature Gas Dynamics*. 2nd ed.
- Bonelli, F., Cutrone, L., Votta, R., Viggiano, A., Magi, V. (2011). "Preliminary Design of a Hypersonic Air-breathing Vehicle". 17th AIAA International Space Planes and Hypersonic Systems and Technologies Conference, 11 - 14 April 2011, San Francisco, California.
- Clark, A.; Wu, C., R.; Mirmirani, M.; Choi, S. (2006). Development of an Airframe-Propulsion Integrated Generic Hypersonic Vehicle Model. 44th AIAA Aerospace Sciences Meeting and Exhibit (AIAA 2006-218).
- Hariramakrishnan, L.; Nehru, K.; Sangeetha, T. (2017). Performance analysis of scramjet inlet. *Imperial Journal of Interdisciplinary Research*, v. 3.
- Heiser, W.; Pratt, D.; Daley, D.; Mehta, U. (1994) *Hypersonic Airbreathing Propulsion*. AIAA Education Series. ISBN 1-56347-035-7. <https://doi.org/10.2514/4.470356>
- Moeckel, W. E., Weston, K. C. (1958) *Composition and thermodynamic properties of air in chemical equilibrium*. NACA TN-4265. Aug. 1958.
- Moura, A. F., Pinheiro Rosa, M. A. (2013). A computer program for calculating normal and oblique shock waves for airflows in chemical and thermodynamic equilibrium. 22nd International Congress of Mechanical Engineering (COBEM 2013).
- Nagamatsu, H. T., Workman, J. B. and Sheer Jr., R. E. (1960). *Oblique Shock Relations for Air at Mach 7.8 and 7200 R Stagnation Temperature*. Schenectady, NY.
- Srinivasan, S., Tannehill, J. C. and Weilmuenster, K. J. (1987). *Simplified Curve Fits for the Thermodynamic Properties of Equilibrium Air*. NASA RP 1181.
- Tannehill, J. C. and Mugge, P. H. (1974). *Improved Curve Fits for the Thermodynamic Properties of Equilibrium Air Suitable for Numerical Computation Using Time-Dependent or Shock-Capturing Methods*. NASA CR-2470.
- Toro, P. G. P.; Carneiro, R.; Araújo, J. W. S.; Marinho, G. S.; Borba, G. L.; Rego, I. S.; Martos, J. F. A. (2018a). Design and Analysis of a generic scramjet air inlet. 17th Brazilian Congress of Thermal Sciences and Engineering (ENCIT 2018-0751). Águas de Lindóia/SP, Brazil.
- Toro, P. G. P.; Carneiro, R.; Araújo, J. W. S.; Marinho, G. S.; Borba, G. L.; Rego, I. S.; Martos, J. F. A. (2018b). Design of the Generic Scramjet Combustion Chamber. 17th Brazilian Congress of Thermal Sciences and Engineering (ENCIT 2018-0056). Águas de Lindóia/SP, Brazil.

U.S. Standard Atmosphere. (1976). National Oceanic and Atmosphere Administration, National Aeronautics and Space Administration and United States Air Force. Nasa TM-X 74335.

7. RESPONSIBILITY NOTICE

The authors are the only responsible for the printed material included in this paper.

The Authors declare that there is no conflict of interest regarding the publication of this scientific article.

Copyright © 2021 by Paulo G. de P. Toro. Published in 26th International Congress of Mechanical Engineering.